RSC Advances

PAPER

View Article Online
View Journal | View Issue

Cite this: *RSC Adv.*, 2018, **8**, 41782

Facile fabrication of multifunctional fabrics: use of copper and silver nanoparticles for antibacterial, superhydrophobic, conductive fabrics

Hyae Rim Hong, Jooyoun Kim and Chung Hee Park *

This study aims to develop a multifunctional fabric for antibacterial, superhydrophobic and conductive performance using a facile fabrication method. Conductive metal particles, copper and silver, were used as antibacterial agents as well as a means to create nanoscale roughness on the fabric surface. Subsequent hydrophobic coating with 1-dodecanethiol produced a superhydrophobic surface. The single metal treatment with Cu or Ag, and the combined metal treatment of Cu/Ag were compared for the multifunctionality. The Cu/Ag treated fabric and the Cu treated fabric showed a bacteriostatic rate ≥ 99% and a sterilization rate ≥ 99% against *S. aureus*, suggesting a higher antibacterial activity against the Gram-positive bacteria. In contrast, the Ag treated fabric showed a lower antibacterial effect regardless of the bacteria type. With regards to conductivity, the single metal treated fabric did not exhibit conductivity; however the Cu/Ag treated fabric showed a high level conductivity with a surface resistivity of 25.17 ± 8.18 Ω sq^{-1} and 184.38 ± 85.42 Ω sq^{-1} before and after hydrophobic coating, respectively. Fabrics treated with Cu and Cu/Ag particles (with hydrophobic coating) displayed superhydrophobic characteristics with the contact angle of 161–162° and the shedding angle of 7.0–7.8°. The air permeability decreased after the particle treatment as the particles blocked the pores in the fabric. However, the water vapor permeability and tensile strength were not significantly affected by the particle treatment. This study is significant in that a multifunctionality of antibacterial effect, superhydrophobicity, and conductivity was achieved through the facile processes for metal nanoparticle attachment and hydrophobic coating. The multifunctional fabrics produced in this study can be practically applied to self-cleaning smart clothing, which has reduced laundering need, without hygiene concerns.

Received 8th October 2018
Accepted 29th November 2018

DOI: 10.1039/c8ra08310j

rsc.li/rsc-advances

Introduction

Antibacterial effects can appear by biocidal activity that kills bacteria and/or biostatic activity that prevents bacterial growth.[1] Benefits from an antibacterial finish include the protection from bacterial pathogens and reduction of odor development by hindering bacterial decomposition of soils.[2] For a biocidal antibacterial finish, fabrics can be treated with biocidal chemicals such as quaternary ammonium compounds,[3,4] *N*-halamines,[5] chitosan,[6,7] polybiguanides,[8] triclosan,[9] metal nanoparticles,[10,11] and natural-source plant extracts.[12] Among the biocides, metal ions react with the thiol groups (–SH) of proteins in the bacterial cell wall,[13] effectively destroying bacterial activity. When metal particles are treated onto fabrics for an antibacterial effect, fabrics also gain conductivity.[14]

For biostatic effect, fabrics can be treated for anti-biofouling so that bacterial attachment to the surface is circumvented.[1] Anti-fouling effect can be obtained from a superhydrophobic fabric that has the self-cleaning ability. The superhydrophobic surface, which shows a static water contact angle higher than 150° and a shedding angle lower than 10°,[15] can be designed by lowering the surface energy and implementing micro-nanoscale roughness.[16] For fabricating such a surface, various techniques have been employed including plasma etching,[17,18] chemical etching,[19,20] nanoparticle attachment[21,22] and polymerization.[23] As fabrics have micrometer scale roughness coming from fibers, addition of nanoparticles would form micro/nano-sized dual scale roughness,[24] and further processing with a low surface energy compound would make a superhydrophobic, possibly self-cleaning surface.[25]

While it is expected that such a fabric would have the reduced laundering, hygiene concern still remains.[26] When bacteria accumulate onto fabrics, a biofilm[27] can form, which leads to producing odor, discoloration, and fabric deterioration.[2] Addition of antibacterial functions to the self-cleaning fabric would resolve the hygiene concern for reducing laundering needs. On the other side, a self-cleaning function may lengthen the service life of antibacterial activity through reduced bacterial attachment. Moreover, the hydrophobic coating layer may enhance the durability and service life of antibacterial function through the controlled release of biocides.[28] While the hydrophobic coating could prevent the direct contact of antibacterial agents, metal

Department of Textiles, Merchandising and Fashion Design, Seoul National University, Seoul, 08826, Republic of Korea. E-mail: junghee@snu.ac.kr

nanoparticles were still effective after coating, releasing metal cations and active oxygens.[29–31]

Extensive research have been conducted on the antibacterial effect by the single treatment of silver or copper nanoparticles, investigating its optimal process conditions including particle concentration, particle size and shape.[30,32–34] However, little study was done on the combined effect of both silver and copper nanoparticles. In this study, silver and copper nanoparticles were used to achieve antibacterial and conductive function, and to form the nano-scale roughness necessary for the super-hydrophobicity. Polyester fabric was employed to achieve the multifunctional effect by means of combined attachment of metal nanoparticles and hydrophobic coating. Polyester is one of the mostly prevalently used textile materials for outer garment. Compared to cotton fabrics, polyester fabrics are more difficult to be cleaned for oily soils in a water-based washing system. The remaining soils on fabrics can provide a beneficial environment for bacterial growth, causing adverse hygiene problems. Therefore, this study employed polyester to develop multifunctional fabrics, aiming to solve hygiene problems by implementing antibacterial and superhydrophobic functions on polyester fabrics. To improve the bonding between nanoparticles and fabrics, a polydopamine layer was polymerized onto the fabric surface prior to the nanoparticle treatment. The multifunctional effects of antibacterial activity, conductivity, and superhydrophobicity were analyzed based on treatment conditions, and the interplay between treatments was discussed in relation with the functional effectiveness.

Experimental

Materials

This study used samples of 100% polyester plain fabrics (Young Poong Filltex Co., Ltd., South Korea) with a weight of 101.4 g m^{-2}, a thickness of 0.19 mm, and a yarn count (in inch × inch) of 75d/72f (warp) and 150d/144f (weft). All samples were scoured in an aqueous solution with 5 g l^{-1} of sodium dodecylbenzene sulfonate and 5 g l^{-1} of sodium carbonate in 1 : 30 liquor ratio at 50 °C.

Dopamine hydrochloride was purchased from Sigma Aldrich (USA), and hydrazine monohydrate was obtained from Junsei Chemical (Japan). For water vapor transmission rate test, calcium chloride for U-tube (for moisture measurement, Kanto Chemical Co., Inc., Japan) was used. Ammonium hydroxide, ethanol, copper(II) acetate monohydrate, silver nitrate standard solution (1 N and 0.1 N), 1-dodecanethiol, sodium dodecylbenzene sulfonate, sodium carbonate anhydrous (>99.0%) and other chemicals were obtained from Daejung Chemicals & Metals (South Korea).

Surface treatment of fabrics

Fig. 1 shows an overview of the multifunctional treatment for antibacterial activity, conductivity, and superhydrophobicity. Polydopamine was polymerized on a polyester fabric to introduce hydroxyl groups (–OH), which will combine with the metal nanoparticles on the fabric surface. For antibacterial/conductive treatment, single or combined nanoparticles of copper and silver was attached to fabric surfaces. Subsequent hydrophobic coating with 1-dodecanethiol produced superhydrophobic surface.

Polymerization of polydopamine. A 0.01 mol of ammonium hydroxide was added to 30% v/v ethanol/water solution and stirred with the fabric sample at 200 rpm at room temperature for 30 min. Then dopamine hydrochloride was added to the solution making a concentration of 0.01 M, then the solution was stirred at 200 rpm at room temperature for 24 h. The sample with a polydopamine layer was washed with distilled

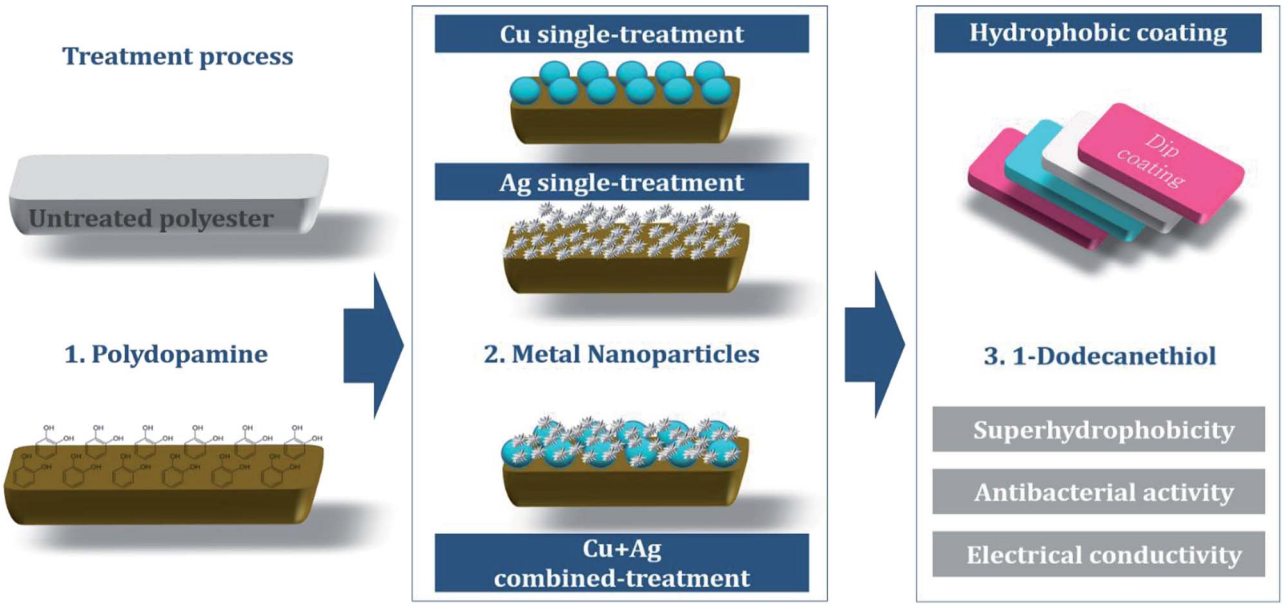

Fig. 1 Overview of surface treatment of polyester fabrics.

water and ethanol before being dried in an oven at 60 °C for 1 h.[35]

Treatment with metal nanoparticles. For the Cu single treatment condition, copper(II) acetate monohydrate was added to 100 ml of distilled water to produce 0.2 M of copper acetate aqueous solution, then the polydopamine-treated sample was immersed. The reducing agent, hydrazine monohydrate, was added to make the molar concentration ratio of 1 : 20 with copper acetate aqueous solution, and then the sealed solution was reacted at room temperature for 8.5 h. The treated sample was washed until the rinsing water remained clear, then dried at 60 °C for 1 h (Fig. 2).

For the Ag single treatment, silver nitrate standard solution (1 N) was diluted in distilled water to produce 100 ml of 0.2 M silver nitrate aqueous solution, and the polydopamine-treated sample was immersed. Hydrazine monohydrate as the reducing agent was added the solution in the mole concentration ratio of 1 : 20 with silver nitrate aqueous solution, then remained for reaction at room temperature for 8.5 h. The treated sample was washed in distilled water, and dried at 60 °C for 1 h.

For the combined treatment of Cu and Ag, Cu particles were first introduced following the similar procedure as the Cu single treatment; the polydopamine-treated sample was immersed in a 0.1 M of copper(II) acetate solution with hydrazine monohydrate for 8 h, then rinsed and dried at room temperature. Then the treated fabric was immersed in 100 ml of 0.1 M silver nitrate solution with stirring at 200 rpm for 30 min. The treated fabric was rinsed with distilled water, and dried at 60 °C for 1 h.[36]

Hydrophobic coating. For hydrophobic coating, 1-dodecanethiol with a low surface energy was added to the solvent ethanol to produce 2% v/v solution. The fabric sample was fully immersed in the solution at room temperature for 30 s.[37]

The sample codes for different treatments are as follows: UT for untreated polyester, D for polydopamine treatment, Cu for Cu single treatment, Ag for Ag single treatment, and H for hydrophobic treatment. The concentrations for nanoparticle treatment are noted in codes (Table 1).

Characterization

Morphologies and chemical compositions. The surface morphologies of fabric samples were analyzed with Field-Emission Scanning Electronic Microscopy (FE-SEM; AURIGA, Carl Zeiss, Germany), and the chemical composition changes were analyzed with Energy Dispersive Spectrometer (EDS; XFlash® FlatQUAD 5060F, Bruker, Germany). Prior to FE-SEM and EDS analysis, the sample surface was coated with platinum at 30 mA for 200 s using a sputter coater (EM ACE200, Leica, Austria). The average diameter of the metal nanoparticles treated with the sample was measured at a 30 000× magnification with FE-SEM. For measurement of particle diameters, five SEM images from different locations were used and from each image, ten non-aggregated nanoparticles were randomly chosen for measurement, and the length of the longest part in particle was measured as diameter of particles assuming them to be spherical. An X-ray Photoelectron Spectroscopy (XPS, AXIS-His, KRATOS, UK) analysis was conducted to confirm changes in surface chemical compositions of the samples with metal nanoparticle treatment and hydrophobic coating.

Add-on ratio. Add-on ratios of the sample with different treatments were measured after samples are conditioned for 24 h at 20 °C and 65% RH. The sample weight was measured using an analytical scale (PAG214C; OHAUS Corporation, UK), and the add-on ratio (%) of treated sample was calculated as follows:

$$\text{Add-on ratio}(\%) = \frac{W_a - W_b}{W_b} \times 100,$$

where W_a is the sample weight after treatment and W_b is the untreated sample weight. An average of 10 samples was recorded.

Antibacterial activity. The antibacterial activity of the samples was tested by the Korea Apparel Testing and Research Institute (KATRI) for *Klebsiella pneumoniae* (American Type Culture Collection no. 4352), a Gram-negative bacterium, and *Staphylococcus aureus* (*Staphylococcus aureus* strain 209, American Type Culture Collection no. 6538), a Gram-positive bacterium. These tests were conducted in accordance with the

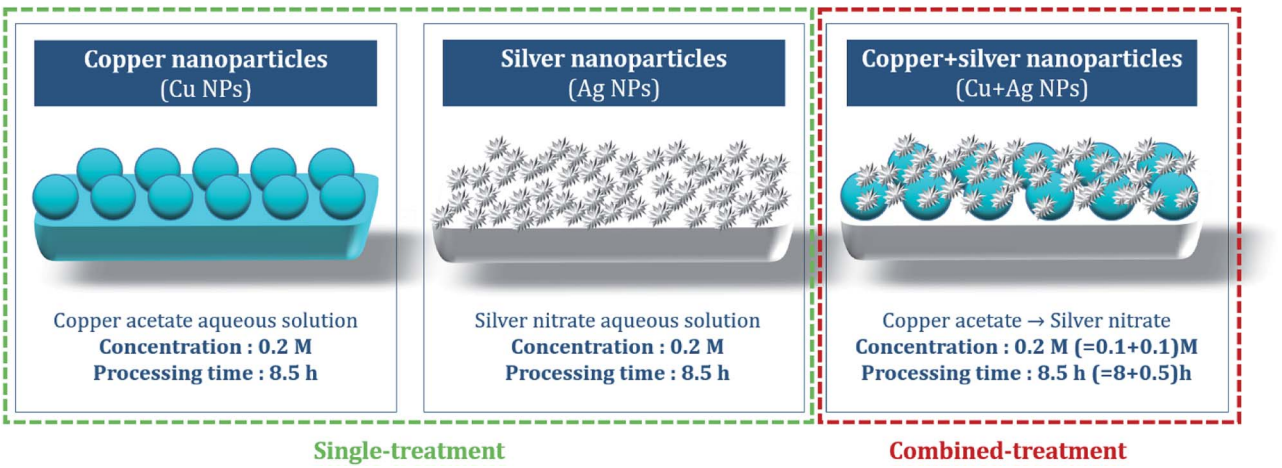

Fig. 2 Schematic illustrations of different metal nanoparticle treatments.

Table 1 Sample codes and description of the process

		Nanoparticle treatment		
	Polydopamine	$Cu(CH_3COO)_2$	$AgNO_3$	Hydrophobic coating
Sample codes	D	Cu	Ag	H
UT	—	—	—	—
H	—	—	—	Treated
D	Treated	—	—	—
D-0.2Cu	Treated	0.2 M	—	—
D-0.2Cu-H	Treated	0.2 M	—	Treated
D-0.2Ag	Treated	—	0.2 M	—
D-0.2Ag-H	Treated	—	0.2 M	Treated
D-0.1Cu-0.1Ag	Treated	0.1 M	0.1 M	—
D-0.1Cu-0.1Ag-H	Treated	0.1 M	0.1 M	Treated

method prescribed for testing the antibacterial activity of textile materials, Korean Industrial Standards (KS) K 0693: 2016.

Fabric samples of 0.4 g for the treated and control were put separately into glass containers and inoculated with 0.2 ml of test bacteria. As the control sample, a standard cotton cloth was used. The glass containers were then sealed and cultured at 37 °C for 18 h. After the culture, 20 ml of a neutralization solution at 0 °C was added to the sample containers and the bacteria attached to the samples were separated. The extracted bacterial solution was diluted in a saline solution and 1.0 ml of this solution was extracted and cultured on a plate culture medium at 37 °C for 24 h. The viable cell count was calculated to two significant digits using the following equation:

$$M = Z \times R \times 20,$$

where M denotes viable cell count, Z denotes colony count, R denotes the dilution factor, and 20 is the amount of the saline solution for extract. Based on the viable cell count, the sterilization rate and bacteriostatic rate of the samples were calculated as follows:

$$\text{Sterilization rate}(\%) = \frac{M_a - M_c}{M_a} \times 100,$$

$$\text{Bacteriostatic rate}(\%) = \frac{M_b - M_c}{M_b} \times 100,$$

where M_a is the viable cell count of the control sample immediately after inoculation, M_b is the viable cell count of the control sample after culture for 18 h, and M_c is the viable cell count of the treated sample after culture for 18 h. The average of three repetitions was used.

The concentrations of the bacterial solution inoculated to the samples are listed below in Table 2. The concentration of bacterial solution varies by the test time; since the antibacterial activity tests were performed at three different time frames, the concentrations of the inoculated bacterial solution were varied depending on the test time. In every test, tween 80, a nonionic surfactant, was added at 0.05% of the bacterial solution so that the bacterial solution would be wetted to the sample.

Conductivity. When the resistance of a sample with a length of l and a cross-sectional area of A is R, the electric conductivity κ (kappa) is defined as follows:

$$\kappa\ (\mathrm{S\ m^{-1}}) = \frac{l}{A \times R}$$

The surface resistivity was measured using a DC milliohm meter (GOM-804, GW Instek Co., Taiwan) in accordance with the American Association of Textile Chemists and Colorists (AATCC) 76-1995. Resistance was measured by vertically applying a 10 N load to a 1 kg jig in which copper terminals in 20 mm × 30 mm were placed at 20 mm intervals on the sample (6 cm × 10 cm). The surface resistance was calculated as follows:

$$R_S = R \times \left(\frac{w}{d}\right),$$

where R_S is surface resistance ($\Omega\ \mathrm{sq^{-1}}$), R is the measured resistance (Ω), d is the distance between two terminals, and w is the width of each terminal. In this study, the distance between terminals (d) was 20 mm and the terminal width (w) was 30 mm. The surface resistance (R_S) was determined by multiplying the measured resistance (R) by 1.5.

Table 2 The concentration of the bacteria inoculated onto the samples

	Concentration of the bacteria (CFU ml^{-1})	
Strains	*Staphylococcus aureus* ATCC 6538	*Klebsiella pneumoniae* ATCC 4352
UT	1.3×10^5	0.7×10^5
H	1.0×10^5	1.2×10^5
D	1.0×10^5	1.2×10^5
D-0.2Cu	0.7×10^5	1.2×10^5
D-0.2Ag	0.7×10^5	1.2×10^5
D-0.1Cu-0.1Ag	1.3×10^5	0.7×10^5
D-0.2Cu-H	0.7×10^5	1.2×10^5
D-0.2Ag-H	0.7×10^5	1.2×10^5
D-0.1Cu-0.1Ag-H	1.3×10^5	0.7×10^5

Surface resistance was measured 5 times at the center and 4 corners on the front and back, and the average was used. For each treatment, the surface resistance was averaged for eight samples. Since resistances greater than 5 MΩ cannot be measured, the corresponding samples were marked "unmeasurable".

Superhydrophobicity. To evaluate surface wettability, water static contact angle and shedding angle were measured using an optical tensiometer (Theta Lite, KSV Instruments Ltd., Finland). The sample was determined to be superhydrophobic if its contact angle was greater than 150° and the shedding angle was less than 10°.

For contact angle measurement, a 3.3 ± 0.3 μl of distilled water was dropped vertically from a height of 1 cm to the sample surface, and the contact angle after 1 s was measured. The contact angle was determined by averaging the right and left angles of the water drop. For each treatment, a total of 25 measurements were averaged.

For the shedding angle, the distilled water of 12.5 ± 0.2 μl dropped vertically from a height of 1 cm to the sample surface, and the minimum angle of sample stage at which the water drop rolls down 2 cm was measured. The slope of the stage was increased in 1° steps and 20 different samples were averaged for each treatment.

Evaluation of breathability and the water vapor permeability. The breathability of the sample was measured by the air permeability tester (FX 3300, Textest AG Co., Switzerland) in accordance with the American Society for Testing and Materials (ASTM) D 737-04, standard test method for air permeability of textile fabrics. For measurement, a sample in 12 cm × 12 cm was conditioned at 20 °C and 65% RH for 24 h and a pressure of 125 Pa was applied. For each treatment condition, three different samples were measured repeatedly. The value was expressed as CFM (cubic feet per minute).

The water vapor permeability of the sample was measured in accordance with KS K 0594:2015, test method for water vapor permeability of textiles. A fabric sample with a 7 cm diameter was fixed on a water-permeable cup containing 33 g of calcium chloride at 40 °C, 90% RH for 1 h, maintaining a 3 mm distance between the sample and the calcium chloride. The mass change (g) was measured after a predetermined time to calculate the water vapor permeability as the following. The average of three tests was used.

$$P = \frac{a_2 - a_1}{S},$$

where P denotes the water vapor permeability [g $(m^2\ h)^{-1}$]; $a_2 - a_1$ denotes the mass change (g h^{-1}) of the water-permeable cup after 1 h; S is the area (m^2) of the sample exposed to the moisture absorbent.

Evaluation of tensile strength. Tensile strength was measured by the strip method of ASTM D5035 using a universal testing machine (Instron-5543, Instron Co., USA). The sample of 2.5 cm × 20 cm was preconditioned for 24 h at 20 °C and 65% RH, then the tensile property was measured with the clamp interval of 7.6 cm, a load of 1 kN, and a load rate of 300 ± 10 mm min^{-1}.

Results and discussion

Surface morphology

From SEM images, the samples treated with metal nanoparticles had dual-scale roughness at the surface while the untreated sample (UT) had only micro-scale roughness by the fibers and yarns with no nanoscale protrusions on them (Fig. 3 and 4). The size and the morphology of nanoparticles from the treated samples varied by the metal type and treatment conditions.

Diameters of metal nanoparticles were measured from the SEM images of 30 000× magnifications. Overall, silver nanoparticles formed smaller spherical crystals than copper particles. The average diameter of the spherical Ag particles on the D-0.2Ag-H sample was approximately 215 ± 21 nm and that of Cu particles on the D-0.2Cu-H was approximately 788 ± 50 nm. The silver cations (Ag^+) have an oxidation number of +1 in silver nitrate ($AgNO_3$) solution, whereas the copper cations (Cu^{2+}) have an oxidation number of +2 in copper acetate $[Cu(CO_2CH_3)_2\cdots H_2O]$ solution; therefore, copper cations have a greater ability to attract electrons than silver cations, forming more bonds with particles and producing particles in larger diameters.

Surface chemical composition

The elements comprising the nanoparticles attached to the surface were mapped and discerned through EDS. It should be noted that the EDS obtains information from the surface rather than the bulk of the sample. The ratio of atoms comprising the elements was measured in spectrums (Fig. 5). Carbon and oxygen are originated from polyester fabrics and polydopamine,[38] sulfur was formed from 1-dodecanethiol treatment.[26,37,39] Copper element accounted for 22.27% from the Cu single treatment sample, and silver accounted for 13.18% from the Ag single treatment sample based on the number of atoms detected on the surface. For the combined treatment of Cu and Ag(D-0.1Cu-0.1Ag-H), copper and silver accounted for 0.50% and 21.30%, respectively. We could see that since silver nanoparticles were bound onto the surface of copper nanoparticles covering them with silver, a larger percentage of silver than actually existing was obtained.

Due to the fact that sulfurs were detected together in the area of metals, it is evident that the thiol groups (–SH) of 1-dodecanethiol are bonded with metal nanoparticles. The 1-dodecanethiol is distributed over the whole surface as it can bond with silver particles, copper particles, and the polydopamine layer.[37,39]

Changes in surface chemical compositions of polyester fabrics with metal nanoparticle treatment and hydrophobic coating were further conducted by XPS analysis (Fig. 6). For UT, the peaks at 284.50 eV, 285.30 eV, 286.37 eV, and 288.55 eV of C 1s spectrum were assigned to C=C, C–C, C–O, and C=O from the polyester, respectively. For D-0.2Cu-H sample, the existence of copper metals (Cu^0) on polyester fabric can be identified by the peaks at 932.69 eV (Cu $2p_{3/2}$) and 952.59 eV (Cu $2p_{1/2}$) of Cu 2p spectrum, and for D-0.2Ag-H sample, silver metals (Ag^0) on polyester fabric can be verified with the peaks at 368.40 eV (Ag $3d_{5/2}$) and 374.40 eV (Ag $3d_{3/2}$) of Ag 3d spectrum.

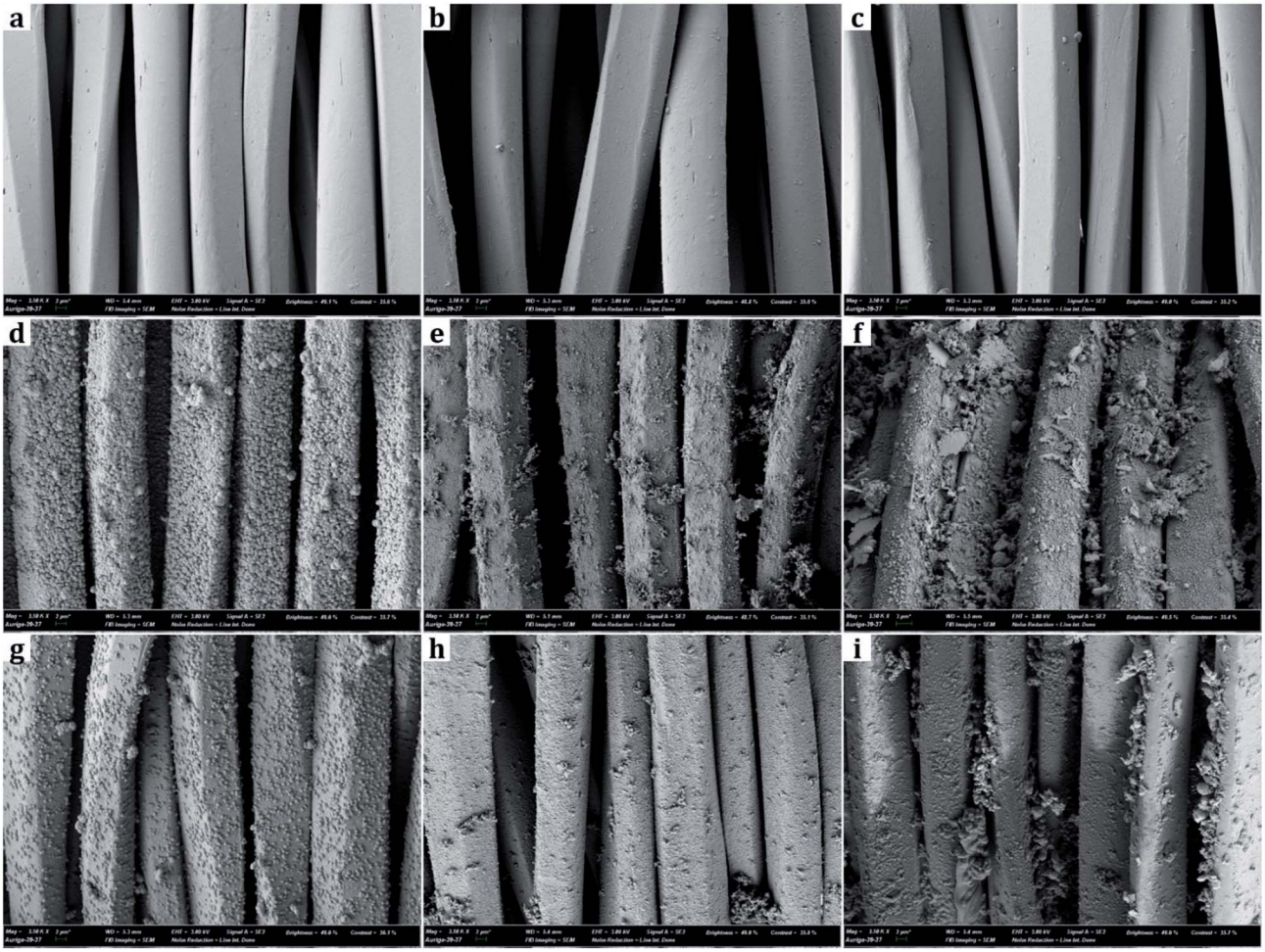

Fig. 3 Scanning electron micrographs images of polyesters at a magnification of ×3500. (a) UT, (b) D, (c) H, (d) D-0.2Cu, (e) D-0.2Ag, (f) D-0.1Cu-0.1Ag, (g) D-0.2Cu-H, (h) D-0.2Ag-H, (i) D-0.1Cu-0.1Ag-H.

For a wide spectrum of D-0.1Cu-0.1Ag-H sample, the peaks for C, O, Cu, Ag, S were detected, and these were matched with EDS results (Fig. 5). The peaks at binding energies of 284.50 eV, 285.30 eV, 286.58 eV, and 288.50 eV of C 1s spectrum originating from C═C, C–C, C–O, and C═O indicated polyester fabric used as the substrate. Presences of nanoparticles of both copper and silver on the sample can be identified from peaks at binding energies of 932.16 eV (Cu $2p_{3/2}$) and 952.06 eV (Cu $2p_{1/2}$) of Cu 2p spectrum and 367.82 eV (Ag $3d_{5/2}$) and 373.82 eV (Ag $3d_{3/2}$) of Ag 3d spectrum. In addition, peaks at binding energies of 161.62 eV (S $2p_{3/2}$) and 162.80 eV (S $2p_{1/2}$) of S 2p spectrum are attributed to chemical bonds between sulfur of 1-dodecanethiol and metal nanoparticles, and 163.43 eV (S $2p_{3/2}$) and 164.61 eV (S $2p_{1/2}$) of S 2p spectrum are ascribed to S–R which makes surfaces have a low surface energy. These XPS results demonstrate that Cu and Ag nanoparticles with hydrophobic coating were successfully bonded to the surface of the polyester.

Metal nanoparticles formation mechanism

For single treatment of nanoparticles, spherical nanoparticles were evenly distributed on the fabric surface in a two-dimensional manner. When the polydopamine-treated sample is immersed in a silver nitrate solution, Ag^+ ions in the solution bond with OH^- groups in the polydopamine layer. As a result, Ag^+ ions aggregate and act as reaction points for growing into silver nanoparticles. The addition of a reducing agent at this time turns the transparent solution to a grayish brown color; the silver cations in the solution receive electrons from the reducing agent and aggregate to reach low energy states. As Ag^+ and electrons aggregate around the reaction points, they grow into spherical silver nanoparticles. The reaction terminates when aggregation no longer exists in the polydopamine layer and silver precipitates are formed in the solution. The same mechanism applies to Cu single treatment; when the polydopamine-treated sample is immersed in a copper acetate aqueous solution, the copper is aggregated when copper cations bound to polydopamine receive the electrons from the reducing agent.

For the combined treatment of Cu and Ag, nanoparticles in different sizes form three-dimensional nano-roughness on the fabric surface. The difference of the standard electrode potential (E°) between copper and silver leads to oxidation–reduction reactions, making bonds between Cu and Ag. The standard electrode potentials of copper and silver at 25 °C and 1 atmosphere are as follows:[14]

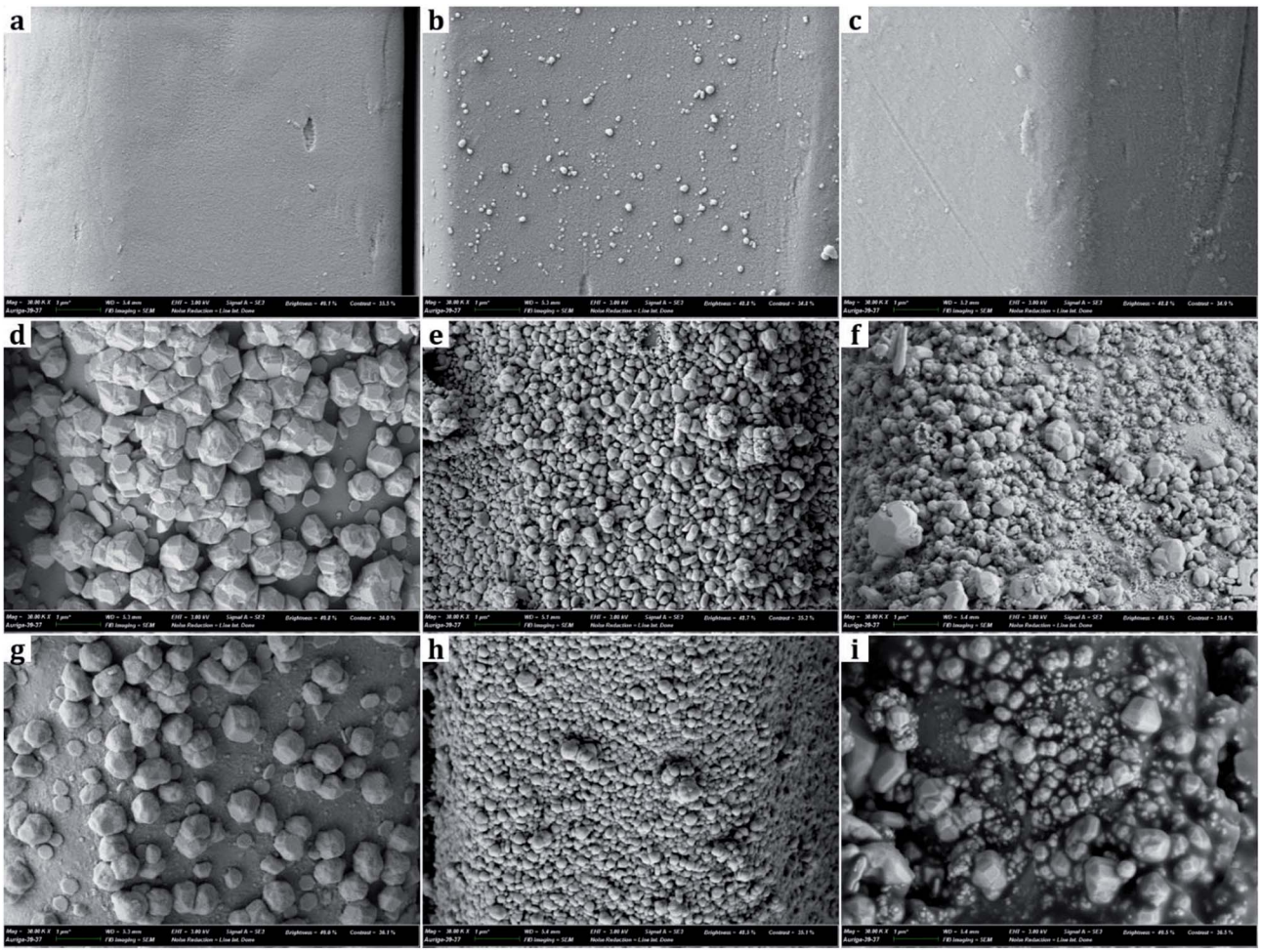

Fig. 4 Scanning electron micrographs images of polyesters at a magnification of ×30 000. (a) UT, (b) D, (c) H, (d) D-0.2Cu, (e) D-0.2Ag, (f) D-0.1Cu-0.1Ag, (g) D-0.2Cu-H, (h) D-0.2Ag-H, (i) D-0.1Cu-0.1Ag-H.

$$Ag^{+}(aq.) + e^{-} \rightarrow Ag(s),\ E^{\circ} = +0.80\ V$$

$$Cu^{2+}(aq.) + 2e^{-} \rightarrow Cu(s),\ E^{\circ} = +0.34\ V$$

Since silver has a higher standard electrode potential, parts of the copper surfaces can be replaced with silver particles by the following reaction:

$$Cu(s) + 2AgNO_3(aq.) \rightarrow 2Ag(s) + Cu(NO_3)_2(aq.)$$

$$Cu(s) + 2Ag^{+}(aq.) + 2NO^{3-}(aq.) \rightarrow 2Ag(s) + Cu^{2+}(aq.) + 2NO^{3-}(aq.)$$

When copper is oxidized and exists as a copper cation in solution, the released electrons combine with the silver cation to form a silver nanoparticle. At this time, the ratio of copper released from the copper nanoparticles and the silver reduced and attached to copper nanoparticles becomes 1 : 2.

$$\text{(Oxidation reaction equation) } Cu \rightarrow Cu^{2+} + 2e^{-}$$

$$\text{(Reduction reaction equation) } 2Ag^{+} + 2e^{-} \rightarrow 2Ag$$

This oxidation–reduction reaction continues until there are no more silver cations to react with on the surface of copper nanoparticles. In this process, the reduced silver nanoparticles are bound to the surface of copper nanoparticles attached to the fabric and form crystals in a three-dimensional manner.

Antibacterial activity

The antibacterial effect of treated fabrics were investigated by the sterilization rate and bacteriostatic rate after 18 h bacterial inoculation (Table 3).

In every sample, the antibacterial effect against the Gram-positive *Staphylococcus aureus* (*S. aureus*, ATCC 6538) was greater than against the Gram-negative *Klebsiella pneumoniae* (*K. pneumoniae*, ATCC 4352). Metal nanoparticles can kill bacteria by directly binding to and destroying cell walls, or by inhibiting the growth of bacteria through interference with the respiratory function of cells.[27] The metal cations and active oxygens released from metal particles penetrate the bacterial

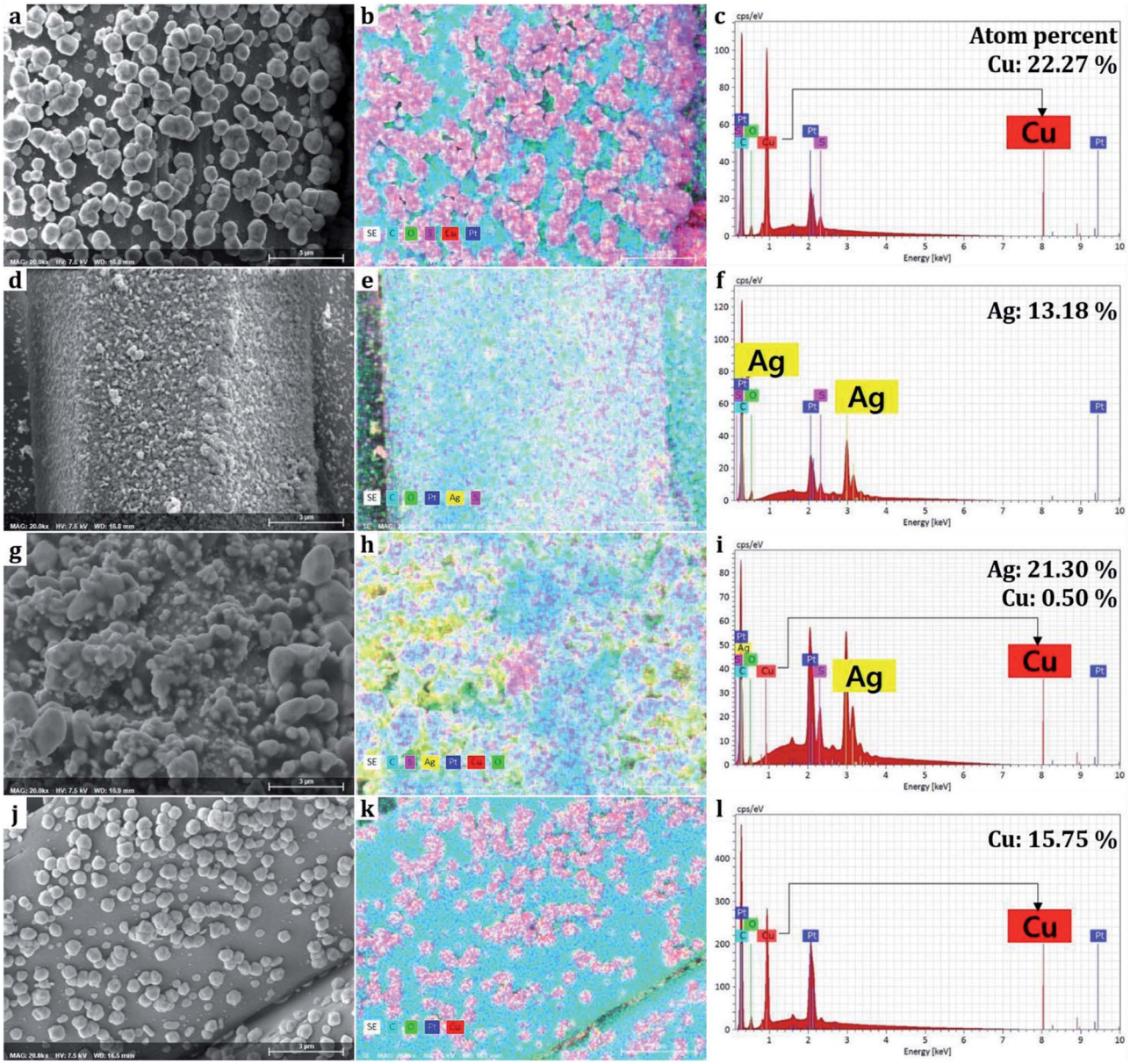

Fig. 5 Surface chemical composition analysis of polyesters by energy dispersive spectrometer at a magnification of ×20 000. (a, d, g and j) SEM images, (b, e, h and k) mappings, and (c, f, i and l) spectrums. (a, b and c) Cu single-treated polyester (D-0.2Cu-H), (d, e and f) Ag single-treated polyester (D-0.2Ag-H), (g, h and i) Cu/Ag treated polyester (D-0.1Cu-0.1Ag-H) and (j, k and l) only Cu treated polyester before Ag treatment (D-0.1Cu). Different colors indicate different elements such as: carbon (C) in light blue; oxygen (O) in light green; sulfur (S) in pink; copper (Cu) in red; silver (Ag) in yellow; and platinum (Pt) in blue.

cell walls and combine with the thiol groups (–SH) of cells to attack the cell functions. Also, the metal cations combine with sulfur and phosphorus of DNA and destroy the cloning function which prevents the growth of bacteria.[40] For Gram-negative bacteria, the phosphorus of phospholipid of the external membrane react with metal cations, decreasing the metal cations passing through the cell walls and weakening the antibacterial reaction. On the other hand, Gram-positive bacteria consist of a single layer of peptidoglycan, and do not have external membranes to react with metal cations. Thus, a higher concentration of metal cations can attack the Gram-positive bacteria, leading to a higher antibacterial effect.

The Cu/Ag treated sample without hydrophobic coating showed: sterilization rate ≥ 99.8% against *S. aureus*; sterilization rate ≥ 95.7% against *K. pneumoniae*; bacteriostatic rate ≥ 99.9% against both bacteria. The fabrics with Cu single treatment and Ag single treatment without hydrophobic coating showed a bacteriostatic rate ≥ 99.9%, and a sterilization rate ≥ 99.8% against *S. aureus*, and a bacteriostatic rate ≥ 99.9% against *K. pneumoniae*. The combined metals with Cu and Ag resulted in a higher sterilization rate against *K. pneumoniae* than the Cu single treatment. In Rajavel *et al.*'s study,[41] the antibacterial activity of silver nanoparticles increased as the surface area of metals that can come into contact with bacteria increased. Likewise, the difference in

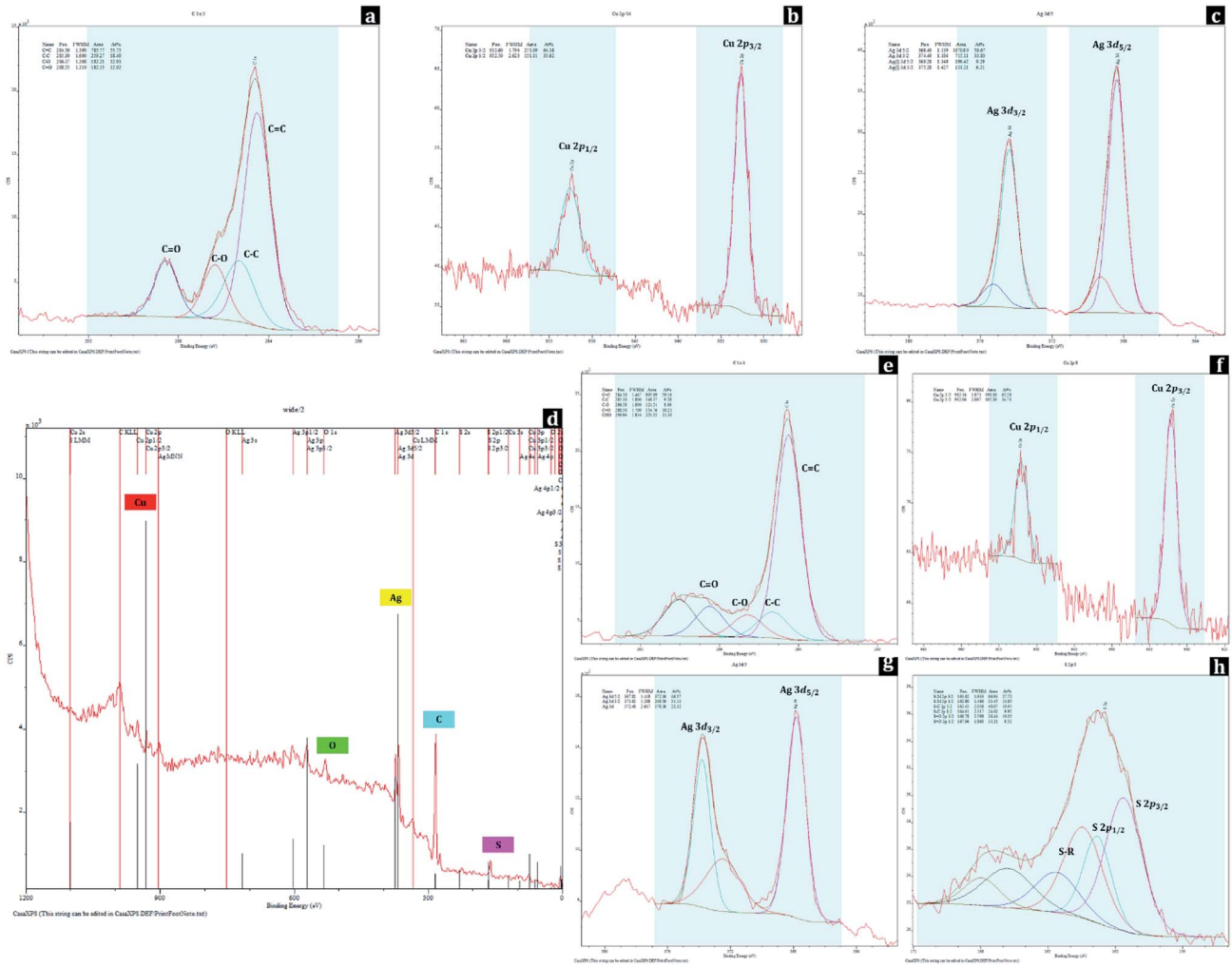

Fig. 6 Surface chemical composition analysis of polyesters by XPS analysis. (a) C 1s spectrum of untreated polyester (UT), (b) Cu 2p spectrum of Cu single-treated polyester (D-0.2Cu-H), and (c) Ag 3d spectrum of Ag single-treated polyester (D-0.2Ag-H). (d) The wide spectrum, (e) C 1s spectrum, (f) Cu 2p spectrum, (g) Ag 3d spectrum and (h) S 2p spectrum of Cu/Ag treated polyester (D-0.1Cu-0.1Ag-H).

antibacterial activity between the single metal treatment and dual metal treatment in this study may be attributed to the difference in surface area for 2D single metal treatment and 3D dual metal treatment. The larger surface of Cu/Ag treated surface would have more released cations that would be in contact with bacterial, showing the higher antibacterial effect.

Table 3 Antibacterial activity of polyesters with different treatments[a]

Strains	Number of bacteria (CFU)			
	Staphylococcus aureus ATCC 6538		*Klebsiella pneumoniae* ATCC 4352	
Antibacterial activity (%)	Sterilization rate	Bacteriostatic rate	Sterilization rate	Bacteriostatic rate
UT	—	94.3	—	31.0
H	8.7	99.6	—	2.6
D	98.5	99.9	—	71.9
D-0.2Cu	>99.8	>99.9	—	99.9
D-0.2Ag	>99.8	>99.9	—	99.9
D-0.1Cu-0.1Ag	>99.8	>99.9	>95.7	>99.9
D-0.2Cu-H	>99.8	>99.9	—	99.5
D-0.2Ag-H	88.1	99.9	—	91.0
D-0.1Cu-0.1Ag-H	99.4	99.9	—	99.9

[a] '—' indicates that it is impossible to measure the sterilization rate.

Meanwhile, the overall antibacterial effect decreased after surface hydrophobic coating. The overall antibacterial effect of D-0.2Ag-H was lower than that of D-0.2Cu-H, and D-0.1Cu-0.1Ag-H, because the add-on ratios of D-0.2Ag-H (5.8%) were significantly lower than those of D-0.2Cu-H (30.3%), and D-0.1Cu-0.1Ag-H (31.2%). The relatively lower amount of Ag onto samples (D-0.2Ag-H) might have resulted in the lower level of antibacterial effect for this sample. For Cu/Ag treated surface, the sterilization rate against *S. aureus* decreased slightly to 99.4% after hydrophobic coating and the bactericidal effect against *K. pneumoniae* was lost. The antibacterial action of metal nanoparticles is largely realized through two paths: the direct contact of metal nanoparticles with cell walls, and the indirect attack of cell walls by cations and radicals generated by metal nanoparticles.[42] With the hydrophobic coating, the antibacterial path through direct contact with cell walls is blocked. Consequently, the antibacterial action is realized only through the indirect path where cations or radicals penetrate the polymer layer and attack the cell walls. Thus, the antibacterial effect decreases after surface hydrophobic coating. However, the bacteriostatic rate against both bacteria was 99.9%; this demonstrates that the inhibition of bacterial growth can be sufficiently achieved even with the single mechanism of indirect path.[43]

In addition, it was interesting to note that polydopamine treated polyester (D) showed antibacterial effect. Referring to the previous studies, it is possible that a strong adhesive property of polydopamine layer leads to the rupture of the bacterial membrane damage.[38,44] Further study on the antibacterial effect of polydopamine itself is needed.

Conductivity

With regard to surface resistivity, Cu/Ag combined treatment showed the lowest surface resistivity of $25.17 \pm 8.18\ \Omega\ sq^{-1}$. With hydrophobic coating, the surface resistivity was still maintained as low as $184.38 \pm 85.42\ \Omega\ sq^{-1}$ (Table 4).

On the other hand, no conductivity was observed in all cases of single treatments of metal nanoparticles regardless of the type of metal nanoparticles used and whether or not the surface hydrophobic coating was applied. This is thought to be caused by the difference in the add-on of the metal particles and the difference of exposed area of metals. For a nonconductive fabric to have conductivity, conductive metals must be sufficiently added onto the fabric surface until it reaches the percolation threshold, the critical point at which conductivity increases sharply.[45] Considering that the add-on ratios were 30.3% for D-0.2Cu-H, 5.8% for D-0.2Ag-H, and 31.2% for D-0.1Cu-0.1Ag-H, insufficient amount of Ag nanoparticles onto samples might have resulted in the lack of conductivity for Ag single treatment.

Table 4 Surface resistance of polyesters with different treatments

Sample code	Surface resistance ($\Omega\ sq^{-1}$)
D-0.2Cu	Unmeasurable
D-0.2Cu-H	Unmeasurable
D-0.2Ag	Unmeasurable
D-0.2Ag-H	Unmeasurable
D-0.1Cu-0.1Ag	25.17 ± 8.18
D-0.1Cu-0.1Ag-H	184.38 ± 85.42

Meanwhile, the Cu treated fabric did not show conductivity even though its add-on ratio was similar to that of the Cu/Ag treated fabric. There are two possible reasons for this; the lower conductivity of Cu over silver and the presence of gaps in metal treatment. An EDS of Cu/Ag treated fabric confirmed that the most of surface area consisted of silver (Fig. 5). When the conductivity of metals (σ, $10^5\ \Omega^{-1}\ cm^{-1}$, 295 K) are compared, Ag has higher conductivity ($\sigma = 6.21$) than Cu ($\sigma = 5.88$).[46] Thus, Cu/Ag treated fabric in which silver nanoparticles were exposed on the surface would have higher conductivity than Cu treated fabric. Also, for fabrics to have high conductivity, the pores between adjacent metal nanoparticles must be minimized so that the conductivity of current through particles is continuous. For Cu single treatment, the particles were stacked with pores and gaps between the particles, which cuts off the flow of current and causes a high surface resistivity. In contrast, for the Cu/Ag combined treatment, small sized silver nanoparticles fill the pores between the copper nanoparticles and the empty spaces on the fabric surface, resulting in a smooth flow of currents and higher conductivity.

Superhydrophobicity

Polydopamine treated samples with/without metal nanoparticles absorbed water within a few seconds due to the hydrophilicity of polydopamine and metals. When hydrophobic coating was applied to the particle-treated fabrics, the contact angle increased greatly. According to the Cassie–Baxter theory, as the interface of liquid with air relative to the interface of liquid with solid increases, the static contact angle increases.[47] In other words, a high contact angle indicates that the contact area between the solid and liquid is reduced with the presence of trapped air between the surface roughness. As the presence of roughness is critical in producing superhydrophobic surface, the attachment of metal nanoparticles to fabric, with additional hydrophobic coating, would be beneficial in creating the superhydrophobic surface.

For UT, the static contact angle was $82.1 \pm 4.6°$. With the introduction of nanoparticles and hydrophobic coating, the Cu treated fabric displayed the highest level of hydrophobic characteristic with the contact angle of $162.1 \pm 5.7°$ and the shedding angle of $7.0 \pm 2.7°$. The Cu/Ag fabric gave the contact angle of $161.3 \pm 3.2°$ and shedding angle of $7.8 \pm 1.2°$. The Ag treated fabric showed the lowest level of hydrophobic property among the tested, with the contact angle of $156.9 \pm 3.1°$ and shedding angle of $18.0 \pm 5.1°$ (Fig. 7). The Ag treated surface had a lowest peak-to-valley distance with a smaller size of silver nanoparticles, thus minimizing the interface between the liquid and air. In contrast, the Cu treated surface shows larger height differences between the nano-roughness features. Therefore, when relatively large copper nanoparticles are stacked on the surface, the air-traps between adjacent nanoparticles become large, resulting in a state closer to the Cassie–Baxter model. While the Cu/Ag treatment can also have large air traps as the Cu treatment, the height difference between the roughness was slightly reduced because fine silver particles filled the pores

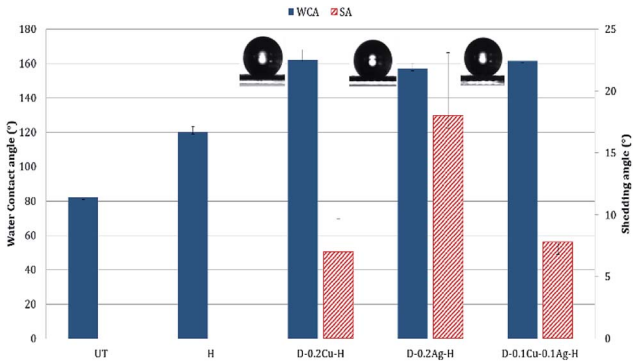

Fig. 7 Water contact angle and shedding angle of polyesters with different treatments.

between the larger copper particles. Thus, the shedding angle of Cu/Ag surface was slightly higher than that of Cu treated surface.

In summary, the shedding angle is affected by both the size and configuration of roughness features. The greater the differences in height and pore size between nanoparticles, the more trapped air pockets are formed at the liquid–solid interfaces. This minimizes the contact area between the liquid and solid, which in turn reduces the shedding angle.

Evaluation of the suitability of the fabric as clothing material

The comfort properties of clothes were evaluated by measuring the air permeability and water vapor permeability. Air permeability and water vapor permeability of polyester with hydrophobic coating (H) were similar to those of the untreated polyester (UT). That is, hydrophobic coating did not block the pores of the fabric and did not change the surface energy noticeably. However, the samples treated with metal and hydrophobic coating together showed reduced air permeability, and it means that the treatment blocked the pores. Among metal nanoparticle treated polyesters, Ag treated sample showed the highest air permeability, followed by Cu treated sample and Cu/Ag treated sample (Fig. 8); this shows that the air permeability is inversely related to the add-on ratio of metal nanoparticles. Because air permeability is greatly affected by the number of pores in fabrics, air permeability of fabrics decreases when the pores of fabrics are blocked with a larger add-on of metal nanoparticles. While the add-on ratios of Cu treated and Cu/Ag treated fabrics were similar, the reduction rate of air permeability (relative to UT) for Cu/Ag treated fabric was considerably higher than for Cu treated fabric; the permeability reduction rate of Cu/Ag was 80.37% and that of Cu was 54.72%. The significantly lower air permeability of Cu/Ag fabric is attributed to the denser accumulation of nanoparticles in 3D configuration. But their vapor permeability kept similar possibly because their surface energy remained almost same and because there was still some pores for vapors to transmit.

For the treated fabrics to be applied to clothing, they should have sufficient strength to endure physical activity and external forces. The tensile strengths of the treated fabrics were compared in Fig. 9. The single metal treated fabrics showed

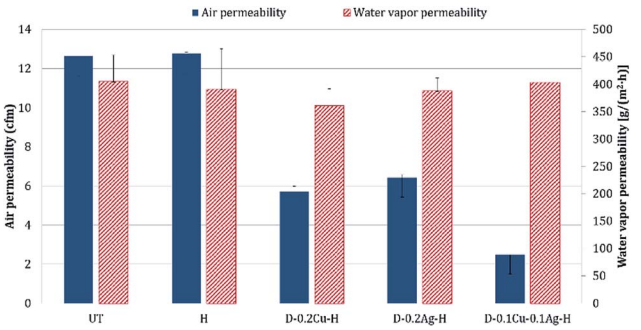

Fig. 8 Breathability of samples with different treatments.

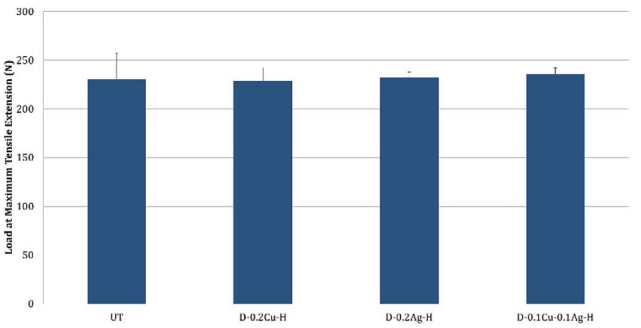

Fig. 9 Tensile strength of polyester fabrics with different metal nanoparticle treatments.

little changes in tensile strength compared to UT. The Cu/Ag treated sample slightly increased the tensile strength by 2.4% relative to UT, resulting from the increased thickness of treated fabrics. For superhydrophobic surface design, such an additive method (particle addition) would have an advantage over etching methods in that tensile strength of the materials can be better maintained.

Conclusions

This study aimed to develop multifunctional fabrics that are conductive, antibacterial and superhydrophobic properties. Such a fabric would overcome the hygiene issue potentially associated with reduced laundering of superhydrophobic, self-cleaning fabrics. As antibacterial agents, silver and copper nanoparticles were used; the introduction of those particles created the roughness that is advantageous for superhydrophobic surface design. Subsequent coating with 1-dodecanethiol lowered the surface energy of the roughened surface, producing superhydrophobic fabrics.

The Cu/Ag treated fabric and the Cu treated fabric showed a bacteriostatic rate ≥ 99% even after hydrophobic coating, and a sterilization rate ≥ 99% against *S. aureus*, suggesting a higher antibacterial activity against the Gram-positive bacteria. In contrast, Ag treated fabric showed the lower antibacterial effect, regardless of the bacteria type. With respect to conductivity, the Cu/Ag treated fabric showed considerably higher conductivity than single metal treated fabrics. Though the conductivity decreased after the hydrophobic coating, the Cu treated and the

Cu/Ag treated fabrics showed excellent superhydrophobicity with the contact angle of 161–162° and shedding angle of 7.0–7.8°, while Ag treated fabric exhibited lower level of hydrophobicity.

The air permeability decreased after metal treatment as the metal particles blocked the pores in the fabric. However, the water vapor permeability was not significantly affected by the particle treatment, as the pore blocking was offset by the facilitated vapor transmission with the metal coating. The tensile properties were maintained or slightly improved after metal particle treatments.

This study is significant in that the multifunctionality with antibacterial effect, superhydrophobicity, and conductivity was achieved through facile processes of nanoparticle attachment and hydrophobic coating. The multifunctional fabric produced in this study can be practically applied as a self-cleaning material with the reduced hygiene concern. This study did not examine the leaching of nanoparticles from the treated fabrics, and the further study on nanoparticle leaching is suggested. Furthermore, it is recommended to explore alternative finishing methods that can negate the potential risk of particle leaching. From the results, the antibacterial effect and conductivity decreased after the hydrophobic coating. A follow-up study is recommended to explore optimal treatment methods for the highest effect of antibacterial activity, superhydrophobicity, and conductivity, by adjusting the process conditions.

Conflicts of interest

There are no conflicts to declare.

Acknowledgements

This work was supported by the National Research Foundation of Korea (NRF) grant funded by the Korea government (Ministry of Science and ICT; Grant No. NRF-2016M3A7B4910940 and NRF-2018R1A2B6003526).

References

1 J. Hasan, R. J. Crawford and E. P. Ivanova, *Trends Biotechnol.*, 2013, **31**, 295–304.
2 E. J. Son, S. G. Son and Y. G. Hwang, *Fiber Technol. Ind.*, 2012, **16**, 65–76.
3 B. Tomšič, E. Ilec, M. Žerjav, A. Hladnik, A. Simončič and B. Simončič, *Colloids Surf., B*, 2014, **122**, 72–78.
4 Y. Fu, J. Jiang, Q. Zhang, X. Zhan and F. Chen, *J. Mater. Chem. A*, 2016, **5**, 275–284.
5 H. Wang, Z.-M. Wang, X. Yan, J. Chen, W.-Z. Lang and Y.-J. Guo, *J. Ind. Eng. Chem.*, 2017, **52**, 295–304.
6 Y.-M. Jeon, T.-W. Son, M.-G. Jeong, M.-J. Kim and H.-S. Lim, *J. Korean Fiber Soc.*, 2003, **40**, 296–306.
7 J. H. Ryu, S. Hong and H. Lee, *Acta Biomater.*, 2015, **27**, 101–115.
8 A. Cazzaniga, V. Serralta, S. Davis, R. Orr, W. Eaglstein and P. M. Mertz, *Wounds*, 2002, **14**, 169–176.
9 C. W. Levy, A. Roujeinikova, S. Sedelnikova, P. J. Baker, A. R. Stuitje, A. R. Slabas, D. W. Rice and J. B. Rafferty, *Nature*, 1999, **398**, 383.
10 S. K. Sehmi, S. Noimark, J. Weiner, E. Allan, A. J. MacRobert and I. P. Parkin, *ACS Appl. Mater. Interfaces*, 2015, **7**, 22807–22813.
11 D. Xu, Y. Su, L. Zhao, F. Meng, C. Liu, Y. Guan, J. Zhang and J. Luo, *J. Biomed. Mater. Res., Part A*, 2017, **105**, 531–538.
12 M.-S. Kim, Y.-J. Shin and J. Jang, *J. Text. Sci. Eng.*, 2013, **50**, 167–173.
13 N. W. Adams and J. R. Kramer, *Environ. Toxicol. Chem.*, 1999, **18**, 2667–2673.
14 P. W. Atkins, L. Jones and K. Kim, *Chemical Principles*, FREEDOM ACADEMY INC., Paju, 2012.
15 C. Neinhuis and W. Barthlott, *Ann. Bot.*, 1997, **79**, 667–677.
16 L. Feng, S. Li, Y. Li, H. Li, L. Zhang, J. Zhai, Y. Song, B. Liu, L. Jiang and D. Zhu, *Adv. Mater.*, 2002, **14**, 1857–1860.
17 H.-s. Kim and C. H. Park, *RSC Adv.*, 2016, **6**, 48155–48164.
18 J. Kim, H.-s. Kim and C. H. Park, *Text. Res. J.*, 2016, **86**, 461–471.
19 M. S. Han, Y. Park and C. H. Park, *Fibers Polym.*, 2016, **17**, 241–247.
20 S. Lee and C. H. Park, *Text. Res. J.*, 2018, **88**, 777–789.
21 Y. Park, C. H. Park and J. Kim, *Text. Res. J.*, 2014, **84**, 1776–1788.
22 S. Jin, Y. Park and C. H. Park, *Text. Res. J.*, 2016, **86**, 1816–1827.
23 C.-H. Xue, X.-J. Guo, J.-Z. Ma and S.-T. Jia, *ACS Appl. Mater. Interfaces*, 2015, **7**, 8251–8259.
24 J. Yang, H. Xu, L. Zhang, Y. Zhong, X. Sui and Z. Mao, *Surf. Coat. Technol.*, 2017, **309**, 149–154.
25 S. Yu, Z. Guo and W. Liu, *Chem. Commun.*, 2015, **51**, 1775–1794.
26 Z. Wang, J. Ou, Y. Wang, M. Xue, F. Wang, B. Pan, C. Li and W. Li, *Surf. Coat. Technol.*, 2015, **280**, 378–383.
27 H. Qian, M. Li, Z. Li, Y. Lou, L. Huang, D. Zhang, D. Xu, C. Du, L. Lu and J. Gao, *Mater. Sci. Eng., C*, 2017, **80**, 566–577.
28 K. Ellinas, D. Kefallinou, K. Stamatakis, E. Gogolides and A. Tserepi, *ACS Appl. Mater. Interfaces*, 2017, **9**, 39781–39789.
29 L. G. Ovington, *Ostomy Wound Management*, 2004, **50**, 1S–10S.
30 M. Wu, B. Ma, T. Pan, S. Chen and J. Sun, *Adv. Funct. Mater.*, 2016, **26**, 569–576.
31 X. Gao and Z. Guo, *J. Bionic Eng.*, 2017, **14**, 401–439.
32 M. R. Nateghi and H. Hajimirzababa, *J. Text. Inst.*, 2014, **105**, 806–813.
33 M. Guzman, J. Dille and S. Godet, *Nanomedicine*, 2012, **8**, 37–45.
34 C.-H. Xue, J. Chen, W. Yin, S.-T. Jia and J.-Z. Ma, *Appl. Surf. Sci.*, 2012, **258**, 2468–2472.
35 B. Shang, Y. Wang, B. Peng and Z. Deng, *J. Colloid Interface Sci.*, 2016, **482**, 240–251.
36 T. Suryaprabha and M. G. Sethuraman, *J. Alloys Compd.*, 2017, **724**, 240–248.
37 W. Zhou, G. Li, L. Wang, Z. Chen and Y. Lin, *Appl. Surf. Sci.*, 2017, **413**, 140–148.

38 E. Faure, C. Falentin-Daudré, C. Jérôme, J. Lyskawa, D. Fournier, P. Woisel and C. Detrembleur, *Prog. Polym. Sci.*, 2013, **38**, 236–270.
39 J. Wang and H. Wang, *Mar. Pollut. Bull.*, 2017, **119**, 64–71.
40 B. Reidy, A. Haase, A. Luch, K. A. Dawson and I. Lynch, *Materials*, 2013, **6**, 2295–2350.
41 K. Rajavel, R. Gomathi, R. Pandian and R. T. Rajendra Kumar, *Inorg. Nano-Met. Chem*, 2017, **47**, 1196–1203.
42 I. S. Hwang, J. Y. Cho, J. H. Hwang, B. M. Hwang, H. M. Choi, J. Y. Lee and D. G. Lee, *Korean J. Microbiol. Biotechnol.*, 2011, **39**, 1–8.
43 N. Durán, M. Durán, M. B. de Jesus, A. B. Seabra, W. J. Fávaro and G. Nakazato, *Nanomedicine*, 2016, **12**, 789–799.
44 C. D. Bandara, S. Singh, I. O. Afara, A. Wolff, T. Tesfamichael, K. Ostrikov and A. Oloyede, *ACS Appl. Mater. Interfaces*, 2017, **9**, 6746–6760.
45 D. Stauffer and A. Aharony, *Introduction to percolation theory: revised second edition*, CRC Press, 2014.
46 V. Palenskis, *World J. Condens. Matter Phys.*, 2013, **3**, 73.
47 A. Cassie and S. Baxter, *Trans. Faraday Soc.*, 1944, **40**, 546–551.